*J Physiol* 590.17 (2012) pp 4335–4350



The Journal of Physiology

# P2Y2 receptor activation opens pannexin-1 channels in rat carotid body type II cells: potential role in amplifying the neurotransmitter ATP

Min Zhang, Nikol A. Piskuric, Cathy Vollmer, and Colin A. Nurse

*Department of Biology, McMaster University, 1280 Main St. West, Hamilton, Ontario L8S 4K1, Canada*

**Key points**

- Carotid body (CB) chemoreceptor complexes consist of receptor type I cells, intimately associated with glia-like type II cells whose function is poorly understood.
- We show that type II cells in the rat CB express gap junction-like proteins, pannexin-1 (Panx-1) channels, which form non-selective pores permeable to ions and large molecules such as ATP, a key CB neurotransmitter.
- Activation of purinergic P2Y2 receptors on type II cells led to a rise in intracellular $Ca^{2+}$, and a prolonged membrane depolarization due to opening of Panx-1 channels.
- In a CB co-culture model, where purinergic P2X2/3-expressing petrosal neurones served as a reporter or biosensor of ATP release, we show that selective activation of P2Y2 receptors on type II cells can lead to ATP release via Panx-1 channels.
- We propose that type II cells may function as amplifiers of the neurotransmitter ATP during chemotransduction, via the mechanism of ATP-induced ATP release.

**Abstract** Signal processing in the carotid body (CB) is initiated at receptor glomus (or type I) cells which depolarize and release the excitatory neurotransmitter ATP during chemoexcitation by hypoxia and acid hypercapnia. Glomus cell clusters (GCs) occur in intimate association with glia-like type II cells which express purinergic P2Y2 receptors (P2Y2Rs) but their function is unclear. Here we immunolocalize the gap junction-like protein channel pannexin-1 (Panx-1) in type II cells and show Panx-1 mRNA expression in the rat CB. As expected, type II cell activation within or near isolated GCs by P2Y2R agonists, ATP and UTP (100 $\mu$M), induced a rise in intracellular [$Ca^{2+}$]. Moreover in perforated-patch whole cell recordings from type II cells, these agonists caused a prolonged depolarization and a concentration-dependent, delayed opening of non-selective ion channels that was prevented by Panx-1 blockers, carbenoxolone (5 $\mu$M) and 4,4′-diisothiocyano-2,2′-stilbenedisulfonic acid (DIDS; 10 $\mu$M). Because Panx-1 channels serve as conduits for ATP release, we hypothesized that paracrine, type II cell P2Y2R activation leads to ATP-induced ATP release. In proof-of-principle experiments we used co-cultured chemoafferent petrosal neurones (PNs), which express P2X2/3 purinoceptors, as sensitive biosensors of ATP released from type II cells. In several cases, UTP activation of type II cells within or near GCs led to depolarization or increased firing in nearby PNs, and the effect was reversibly abolished by the selective P2X2/3 receptor blocker, pyridoxalphosphate-6-azophenyl-2′,4′-disulphonic acid (PPADS; 10 $\mu$M). We propose that CB type II cells may function as ATP amplifiers during chemotransduction via paracrine activation of P2Y2Rs and Panx-1 channels.

(Received 7 May 2012; accepted after revision 19 June 2012; first published online 25 June 2012)
**Corresponding author** C. A. Nurse: Department of Biology, McMaster University, 1280 Main Street West, Hamilton, Ontario L8S 4K1, Canada. Email: nursec@mcmaster.ca

**Abbreviations** BGM, basic growth medium; CB, carotid body; GC, glomus cell cluster; P2Y2R, P2Y2 receptor; PN, petrosal neurone.



DOI: 10.1113/jphysiol.2012.236265

## Introduction

Sensory processing in the mammalian carotid body (CB), the major arterial chemoreceptor organ involved in the peripheral control of breathing, has attracted much attention over the last ∼30 years (Eyzaguirre & Zapata, 1984; Gonzalez *et al.* 1994; Nurse, 2010). It is now well established that clusters of parenchymal type I cells are the transducers for blood-borne chemicals such as low $O_2$ (hypoxia) and high $CO_2/H^+$ (acid hypercapnia). During chemoexcitation these cells depolarize and release a variety of neurotransmitters and neuromodulators that help shape the afferent sensory discharge, ultimately leading to a restoration of blood $P_{O_2}$ and $P_{CO_2}$/pH homeostasis (Gonzalez *et al.* 1994; Iturriaga & Alcayaga, 2004; Nurse, 2005, 2010). Despite controversy about the roles of certain neurotransmitters, there is a consensus that ATP, released from type I cells during chemotransduction, is the principle excitatory neurotransmitter that initiates the chemoreflex by acting on postsynaptic P2X2/3 purinoceptors on the afferent nerve terminals (Iturriaga & Alcayaga, 2004; Nurse, 2005, 2010; Zapata, 2007). Anatomical studies suggest that the chemoreceptor complex forms an intimate association, not only with sinusoidal fenestrated capillaries, but also with glia-like sustentacular or type II cells and their processes, which permeate and ensheath type I cell clusters (McDonald & Mitchell, 1975; Kondo, 2002). While there is evidence that type II cells may act as stem cells capable of differentiating into chemoreceptor type I cells under appropriate conditions (Pardal *et al.* 2007), it remains unclear whether or not they play an active role during chemotransduction. Interest in this idea has emerged with the ultrastructural demonstration of close membrane appositions, with dubious gap junctional morphology, between type I and type II cells (Kondo, 2002), and the localization of functional P2Y2 receptors on type II cells (Xu *et al.* 2003).

In the present study we considered the possibility that within the CB chemosensory complex, the type I cell, sensory nerve ending, and the glia-like type II cell might participate in a tripartite synapse, where purinergic neurotransmission is modulated. Indeed, in the central nervous system (CNS), glial cells are now known to play an active role in synapse integration and may act as modulators of synaptic transmission via gliotransmission at tripartite synapses (Eroglu & Barres, 2010; Parpura *et al.* 2012). Implicated in gliotransmission in the CNS is the recently discovered family of gap junction-like proteins known as pannexins (Huang *et al.* 2007*a*; Iglesias *et al.* 2009; MacVicar & Thompson, 2010). First cloned in 2003, the pannexin family of proteins shares sequence homology with the invertebrate innexins, but no significant homology with vertebrate gap junctional proteins, i.e. connexins (Yen & Saier, 2007; MacVicar & Thompson, 2010). When open, the pannexins form non-selective 'hemichannels' with pores large enough to allow release of large signalling molecules such as ATP from a variety of cell types including erythrocytes, brain astrocytes and neurones (Locovei *et al.* 2006*a*,*b*; Huang *et al.* 2007*a*; Dubyak, 2009; Iglesias *et al.* 2009; MacVicar & Thompson, 2010; Sridharan *et al.* 2010). In contrast to the connexins, which normally require cell–cell contact and are believed to function as hemichannels only under non-physiological conditions such as low extracellular $Ca^{2+}$, pannexin-1 channels function in normal extracellular $Ca^{2+}$ and do not require cell–cell contact (MacVicar & Thompson, 2010). Among the three family members, pannexin-1 (Panx-1) is the best studied and can be activated by mechanical stretch and by extracellular ATP acting via P2Y purinoceptors (Bao *et al.* 2004; Locovei *et al.* 2006*b*).

To address the potential role of pannexins in CB function, we first used immunocytochemistry to localize Panx-1 expression in type II cells *in situ* and in dissociated cell cultures. Given that type II cells were previously shown to express G-protein coupled P2Y2 receptors (Xu *et al.* 2003), it was therefore of interest to investigate whether or not activation of these receptors could lead to opening of Panx-1 channels and consequently release of ATP from these cells. To address the latter, we attempted to reconstruct the tripartite chemosensory complex as a monolayer, using an established co-culture model of glomus cell clusters (GCs), comprising type I and interspersed type II cells, and juxtaposed chemoafferent petrosal neurones, which express ligand-gated P2X2/3 purinoceptors (Zhang *et al.* 2000). This permitted us to investigate whether it was plausible that selective activation of P2Y2 receptors on type II cells with the agonist UTP could induce ATP release, detected using the petrosal neurone as a reporter or biosensor.

## Methods

### Ethical approval

All procedures for animal handling and tissue dissections were carried out according to the guidelines of the Canadian Council on Animal Care (CCAC) and institutional guidelines. The authors have read, and the experiments comply with, the policies and regulations of *The Journal of Physiology* given by Drummond (2009).

### Cell cultures

**Cultures of dissociated rat carotid body.** Juvenile rat pups, 9–14 days old (Wistar, Charles River, Quebec, Canada), were first rendered unconscious by a blow to the back of the head and then killed immediately

by decapitation. Carotid bodies (CBs) were excised bilaterally and dissociated cell cultures prepared according to well-established procedures in this laboratory (Zhong *et al.* 1997, 2000; Nurse & Fearon, 2002). Briefly, the excised CBs were incubated for 1 h at 37°C in an enzymatic solution containing 0.1% trypsin (Sigma-Aldrich, Oakville, Ontario, Canada) and 0.1% collagenase (Gibco, Grand Island, NY, USA), prior to mechanical dissociation and trituration. The resulting cell suspension was plated onto a thin layer of Matrigel (BD Biosciences, Mississauga, Ontario, Canada), applied to the central wells of modified 35 mm tissue culture dishes (Zhong *et al.* 1997). In some experiments, cells were cultured in basic growth medium (BGM) consisting of F-12 nutrient medium supplemented with 10% fetal bovine serum, 1% penicillin–streptomycin, 1% glutamine, 0.3% glucose, and 3 $\mu$g ml$^{-1}$ insulin, as in previous studies (Zhang *et al.* 2000). In other experiments, the medium was changed after 24 h incubation from BGM to one which appeared to enrich the proportion of type II cells in these cultures (our unpublished observations). This latter growth medium (Cosmic-BGM) consisted of 50% BGM plus 50% of modified BGM where 10% fetal bovine serum was replaced with 5% fetal bovine serum and 5% Cosmic calf serum (Hyclone Laboratories Inc, Utah, USA). In the present experiments there were no obvious differences in the properties of type II cells cultured in BGM *versus* Cosmic-BGM. Cultures were grown at 37°C in a humidified atmosphere of 95% air–5% $CO_2$. Patch clamp recordings were usually carried out after CB cells were in culture for 3–6 days; $Ca^{2+}$-imaging experiments were carried out after ∼24 h in culture.

**Carotid body–petrosal neurone co-cultures.** Procedures for preparing co-cultures of dissociated CB cells and petrosal neurones were similar to those described previously (Zhong *et al.* 1997; 2000). Briefly, petrosal ganglia from 9- to 14-day-old rat pups were excised and isolated neurones prepared using combined enzymatic and mechanical dissociation. Co-cultures were obtained by first preparing CB cultures as described above, and then adding an overlay of dissociated petrosal neurones ∼3 days later. Growth conditions were the same for co-cultures as for CB alone cultures.

## Electrophysiology

Nystatin perforated-patch whole cell recording was used to measure membrane potential and ionic currents in CB cells and petrosal neurones as previously described (Zhang *et al.* 2000). Measurements were obtained from single cells with the aid of an Axopatch 1D or a dual headstage MultiClamp 700B patch clamp amplifier and a Digidata 1200 or 1322A analog-to-digital converter (Axon Instruments Inc., Union City, CA, USA), and the data stored on a personal computer. Data acquisition and analysis were performed using pCLAMP software (versions 6.0.2 and 9.0; Axon Instruments Inc.). For multiple comparisons of ionic currents (pA), ANOVA was used and the level of significance was set at $P < 0.05$.

## Solutions and drugs

All recordings were carried out at ∼35°C and the extracellular solution consisted of a bicarbonate/$CO_2$-buffered saline (BBS) of the following composition (mM): NaCl, 115; $NaHCO_3$, 24; KCl, 5; $CaCl_2$, 2; $MgCl_2$, 1; glucose, 10; and sucrose, 12; at pH 7.4, maintained by bubbling 95% air–5% $CO_2$. The BBS used in $Ca^{2+}$ imaging experiments had the following composition (in mM): NaCl, 115; $NaHCO_3$, 24; KCl, 5; $CaCl_2$, 2; $MgCl_2$, 1; and glucose, 5; at pH 7.4, maintained by bubbling 95% air-5% $CO_2$. The pipette solution contained (mM): potassium gluconate, 115; KCl, 25; NaCl, 5; $CaCl_2$, 1; Hepes, 10; and nystatin 300 $\mu$g ml$^{-1}$; at pH 7.2. Agonists were applied by a 'fast perfusion' system utilizing a double-barrelled pipette assembly as previously described (Zhong *et al.* 1997). The following reagents and drugs were obtained from Sigma-Aldrich (Oakville, ON): ATP, UTP, suramin, reactive blue 2; carbenoxolone (CBX), 4,4′-diisothiocyano-2,2′-stilbenedisulfonic acid (DIDS), pyridoxalphosphate-6-azophenyl-2′,4′-disulphonic acid (PPADS).

## Measurements of intracellular free $Ca^{2+}$

Intracellular free $Ca^{2+}$ concentration ($[Ca^{2+}]_i$) was measured using the fluorescent $Ca^{2+}$ indicator, fura-2/AM (Molecular Probes, Eugene, OR, USA) as described in detail elsewhere (Piskuric & Nurse, 2012). Briefly, cells were loaded with 2.5 $\mu$M fura-2/AM diluted in BBS for 30 min at 37°C, and subsequently washed for ∼15 min to remove free dye. Ratiometric $Ca^{2+}$ imaging was performed using a Nikon Eclipse TE2000-U inverted microscope (Nikon, Mississauga, ON, Canada) equipped with a Lambda DG-4 ultra high-speed wavelength changer (Sutter Instrument Co., Novato, CA, USA), a Hamamatsu OCRCA-ET digital CCD camera (Hamamatsu, Sewickley, PA, USA) and a Nikon S-Fluor 40× oil-immersion objective lens with a numerical aperture of 1.3. Dual images at 340 nm and 380 nm excitation (510 nm emission) were acquired every 2 s with an exposure time of 100–200 ms, and pseudocolour ratiometric data were obtained using Simple PCI software v. 5.3 (Hamamatsu). All experiments were performed at 21–23°C while the culture was continuously perfused via a peristaltic pump with BBS bubbled with 5% $CO_2$ at pH ∼7.4. Reagents (e.g. ATP and UTP) were added to the perfusion reservoir

at the required concentration. Data analysis, including estimation of intracellular free $[Ca^{2+}]$, was identical to that described in detail elsewhere (Piskuric & Nurse, 2012).

## Immunofluorescence staining

**Whole mounts.** Juvenile rats (2–3 weeks old) were anaesthetized with sodium pentobarbital (50 mg kg$^{-1}$ I.P.) and perfused through the left ventricle with phosphate-buffered saline (PBS) followed by PBS containing 4% paraformaldehyde. The carotid bifurcation was then excised, cleaned and post-fixed for 2–3 h at room temperature in 4% paraformaldehyde. The tissue was then washed in PBS (3 × 5 min each) and incubated overnight in 30% sucrose at 4°C. Sections (thickness, 18–20 $\mu$m) of the bifurcation containing the CB were cut in a cryostat and collected on glass slides coated with 2% silane (Sigma). After air drying, sections were stored at −20°C until ready for immunostaining. After thawing and rehydration in PBS, sections were incubated overnight at 4°C with primary antisera (see below) diluted in 1% BSA/PBS, 0.5% Triton-X100. Sections were washed 3× in PBS and then incubated in FITC goat anti-rabbit IgG (1:50; Jackson ImmunoResearch Laboratories, West Grove, PA, USA) plus Dylight 594 goat anti-mouse IgG (1:500; Jackson ImmunoResearch Laboratories).

**Cell cultures.** For pannexin-1 (Panx-1) and tyrosine hydroxylase (TH) co-immunostaining, carotid body cultures were washed with warmed PBS and incubated for 15 min in 4% paraformaldehyde at room temperature. After washing 3× in PBS, cultures were incubated overnight at 4°C in mouse anti-TH monoclonal antibody (1:2000; Millipore/Chemicon, Temecula, CA, USA) plus rabbit anti-Panx1 antibody (3 $\mu$g ml$^{-1}$; Invitrogen Canada Inc., Burlington, Ontario, Canada) diluted in 1% BSA–PBS–0.5% Triton X-100. For Panx-1 and mouse glial fibrillary acid protein (GFAP) co-immunostaining, fixation was carried out in 5% acetic acid–95% methanol for 1 h at −20°C. Cultures were then incubated overnight at 4°C in anti-GFAP antibody (1:800; Millipore/Chemicon) plus anti-Panx1 (3 $\mu$g ml$^{-1}$) in 1% BSA–PBS–Triton X-100. All specimens were then washed 3× in PBS before incubation in the dark for 1 h at room temperature in FITC-conjugated goat anti-rabbit IgG (1:50; Jackson ImmunoResearch Laboratories) plus Texas Red-conjugated goat anti-mouse IgG (1:50; Jackson ImmunoResearch Laboratories). After washing 3 times (5 min each), Vectashield (Vector Laboratories, Burlington, Ontario, Canada) was applied to the cultures to prevent photobleaching. No blocking peptides were available for control staining; however, immunostaining was abolished when the primary antiserum was omitted.

## Confocal microscopy

Stained specimens were first examined using standard epifluorescence to identify regions of interest for confocal examination. Confocal images of immunostained cells were obtained using the Leica TCS SP5 II confocal system, equipped with argon (458, 476, 488, 515 nm) and helium–neon (543, 594, 633 nm) lasers, and a 63× oil objective with a 1.4 numerical aperture (Leica). Specimens were scanned in optical sections separated by ∼2 $\mu$m. Data acquisition and adjustment of brightness and contrast were controlled with the aid of LAS AF (version 2.1.2, Leica). Images were cropped and/or rotated in Adobe Photoshop CS3 Extended (version 10.0.1) and figures were compiled in Adobe Illustrator CS3 (13.0.1).

## Reverse transcriptase–polymerase chain reaction (RT-PCR)

A total of 24 whole carotid bodies from 10- to 12-day-old rat pups were isolated and cleaned of surrounding connective tissue. Total RNA was extracted using Bio-Rad Aurum Total RNA Mini kit and RNA was reverse transcribed using Superscript III reverse transcriptase (Invitrogen). Gene-specific primers for rat pannexin-1 (Panx-1) were identical to those used in previous studies (Lai *et al.* 2007), and were synthesized by The Central Facility of the Institute for Molecular Biology and Biotechnology (MOBIX, McMaster University). The following primers for Panx-1 and the house keeping gene (GAPDH) were used and are listed as sequence amplified, 5′ to 3′ upstream primer sequence (forward), 5′ to 3′ downstream primer sequence (reverse), and size of product (bp):

Panx-1, 5′-TTCTTCCCCTACATCCTGCT-3′ 5′-GGTCC ATCTCTCAGGTCCAA-3′, 185;
GAPDH, 5′-TTCACCACCATGGAGAAG GC-3′ 5′-GG CATGGACTGTGGTCAT GA-3′, 230

DNA was amplified in a single round of PCR using High Fidelity Taq DNA Polymerase (Invitrogen). PCR was held at 94°C for 2 min and cycled 35 times. Each cycle consisted of 94°C for 45 s (denaturing), 50°C for 1 min (annealing), and 72°C for 1 min (elongation and extension). This was followed by 10 min final extension at 72°C. PCR products were identified with a 1.8% agarose gel stained with ethidium bromide and viewed under UV illumination. PCR fragments were extracted from the agarose gel using QIAquick Gel Extraction kit (Qiagen) and DNA was sequenced at MOBIX. Sequencing results were analysed by BLAST2 (basic local alignment search tool) a NIH computer software for identification of gene sequences. Sequences were matched to *Rattus norvegicus* Pannexin1 (Genbank accession number NM-199397.1).

## Results

### Expression of pannexin-1 channels in rat carotid body: localization in type II cells *in situ* and in dissociated cell culture

Using confocal immunofluorescence techniques we first investigated the expression of pannexin-1 (Panx-1) channels in tissue sections of 2- to 3-week-old rat carotid body (CB). As illustrated in Fig. 1*A*–*D*, Panx-1 was not expressed in tyrosine hydroxylase (TH)-positive chemoreceptor glomus or type I cells but, consistent with positive type II cell staining, it was strongly expressed in contiguous cells with processes that appeared to ensheath type I cells ($n = 3$). In dissociated CB cultures, type II cells may occur interspersed within glomus cell clusters (GCs), and often as solitary isolated cells near the periphery of the GCs (Nurse & Fearon, 2002; Piskuric & Nurse, 2012). Within GCs in culture, Panx-1 labelled cells with the expected characteristics of type II cells; this labelling pattern was separate and distinct from TH-positive type I cells as exemplified in Fig. 1*E* ($n = 10$). Moreover, type II cells in culture may also occur as solitary, spindle-shaped, elongated cells, immunopositive for the glial-cell marker GFAP (Pardal *et al.* 2007; Piskuric & Nurse, 2012), which co-localized with Panx-1 immunostaining (Fig. 1*F*–*H*; $n = 5$). Consistent with these findings, Panx-1 mRNA was also detected in whole CB extracts using RT-PCR techniques as illustrated in Fig. 6*E* ($n = 3$), though other cell types including endogenous efferent autonomic neurons (Campanucci *et al.* 2012) and red blood cells (Locovei *et al.* 2006*a*; Sridharan *et al.* 2010) are likely to contribute.

### ATP depolarizes and activates an inward current in type II cells

ATP, acting via P2Y purinoceptors and increased cytoplasmic $Ca^{2+}$, is known to cause opening of

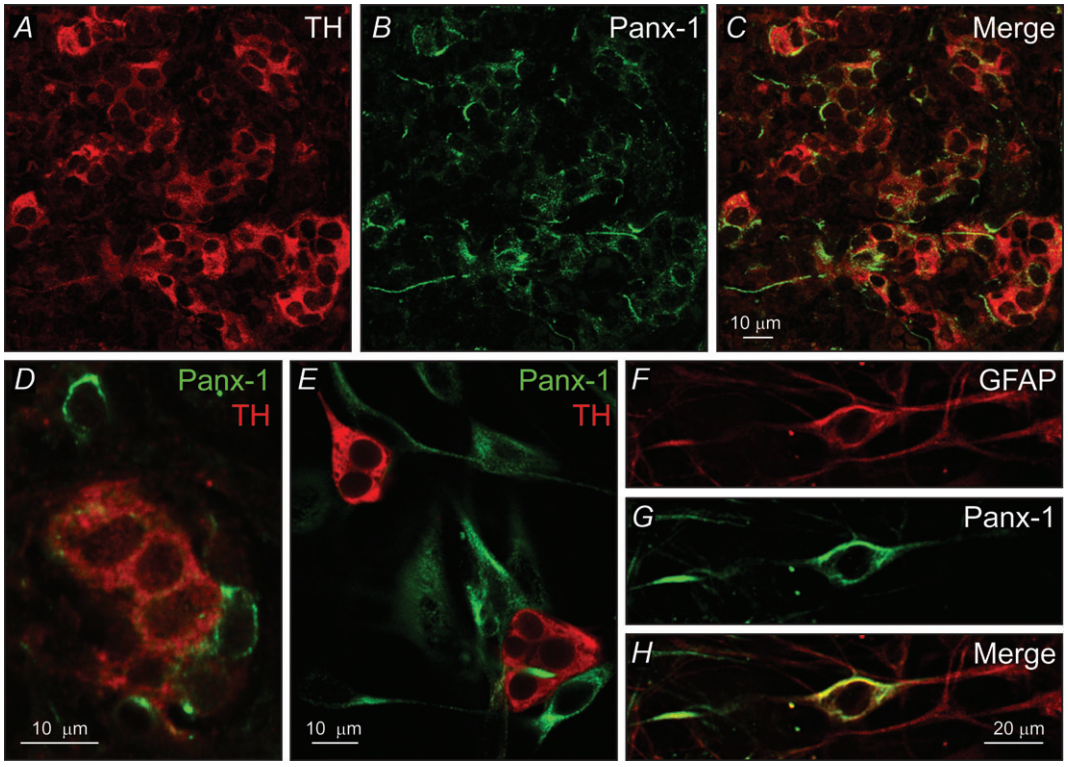


**Figure 1. Confocal images of pannexin-1 (Panx-1) immunostaining of type II cells in tissue sections and dissociated cell cultures of ~2-week-old rat carotid body**
*A*–*C*, a region from a tissue section containing clusters of type I cells stained for tyrosine hydroxylase (TH; red) is shown in *A*; Panx-1 labelling (green) of type II cells is shown for the same microscopic field in *B*, and the overlay is shown in *C*; staining of Panx-1-positive fibres from autonomic efferent neurons (Campanucci *et al.* 2012), may also be present in (*B*). *D*, a high power micrograph from a tissue section showing distinct TH (red) and Panx-1 (green) staining of the soma of type I and type II cells respectively. *E*, region from a dissociated 4-day-old carotid body culture grown in medium (Cosmic-BGM) that enriches for type II cells (see Methods); note separate TH and Panx-1 staining in type I (red) and type II (green) cells respectively. *F*–*H*, a solitary, spindle-shaped type II cell from a 6-day-old culture grown in basic growth medium (BGM) shows positive immunostaining for GFAP (*F*), Panx-1 (*G*), and overlay (*H*).

Panx-1 channels which behave as non-selective, large-conductance plasmalemmal pores permeable to ions and large molecules <1 kDa (Locovei *et al.* 2006*a*; Iglesias *et al.* 2009; MacVicar & Thompson, 2010). Because rat type II cells express P2Y2 receptors whose activation leads to a rise in cytosolic $Ca^{2+}$ (Xu *et al.* 2003; Piskuric & Nurse, 2012), we tested whether ATP could induce Panx-1 channel opening and consequently, membrane depolarization. During perforated-patch whole-cell recording, random sampling within GCs occasionally revealed cells with type II characteristics as observed in earlier studies (Duchen *et al.* 1988). In contrast to receptor type I cells, which were routinely encountered within GCs and showed brief capacitative transients and large voltage-dependent outward $K^+$ currents (Fig. 2*a1*), type II cells were infrequently encountered, often displayed large capacitative transients (Fig. 2*Ba*), and either lacked or showed small, voltage-dependent outward currents (Fig. 2*Ba*, *Ca*). The mean (± SEM) input capacitance and input resistance of type II cells were 24.4 ± 2.4 pF and 987 ± 99.5 MΩ ($n = 10$), respectively. When present within GCs, type II cells had a mean resting potential of −45 ± 3.3 mV (range: −40 to −62 mV; $n = 8$) and depolarized following rapid application of 50 $\mu$M ATP as illustrated in Fig. 2*Bb*, *Cb*. The mean depolarization was 14.4 ± 2.3 mV ($n = 9$), and was accompanied by a conductance increase (Fig. 2*Cb*; see later), suggesting the opening of ion channels at the resting membrane potential. By contrast, type I cells showed no change in membrane potential during application of 50 $\mu$M ATP (e.g. Fig. 2*Ab*), consistent with previous studies from this laboratory showing the lack of effect of ATP over the dose range 10–100 $\mu$M on type I cells cultured alone (Zhang *et al.* 2000; Campanucci *et al.* 2006).

The ATP-induced depolarization in type II cells within GCs arose after a delay where the mean latency was 701.2 ± 290 ms (range: 240–2690 ms; $n = 8$); however its duration was prolonged and variable, usually persisting for several seconds after the stimulus was terminated (Figs. 2*Bb* and *Cb* and 3*A* and *B*). A common feature, exemplified in Fig. 3*A* and *B*, was the complex fluctuations in membrane potential during the depolarization, sometimes leading to a second depolarizing wave after the initial one, and usually after the ATP perfusion was terminated (see also Figs 6*B* and 8). Consistent with the presence of P2 receptors, the ATP-induced depolarization was reversibly inhibited (∼70%) by the non-specific P2 receptor blockers, reactive blue 2 (RB2, 20 $\mu$M; Fig. 3*A*, $n = 6$) and suramin (100 $\mu$M; Fig. 3*B*, $n = 5$).

We also tested the effects of ATP on identifiable spindle-shaped, solitary type II cells that were situated close to, but isolated from adjacent GCs (see Fig. 1*F–H*). After confirming their identity using the electrophysiological profile described in Fig. 2*Ba* and *Ca*, the ATP-induced currents under voltage clamp were used to construct a dose–response relation. As illustrated in Fig. 4*A* and *B*, increasing doses of ATP evoked slowly developing inward currents at –60 mV (holding potential) with an $EC_{50}$ of ∼34 $\mu$M ($n = 5$). The latency of the ATP-induced current appeared much longer (∼10×) in these solitary type II cells, compared to type II cells

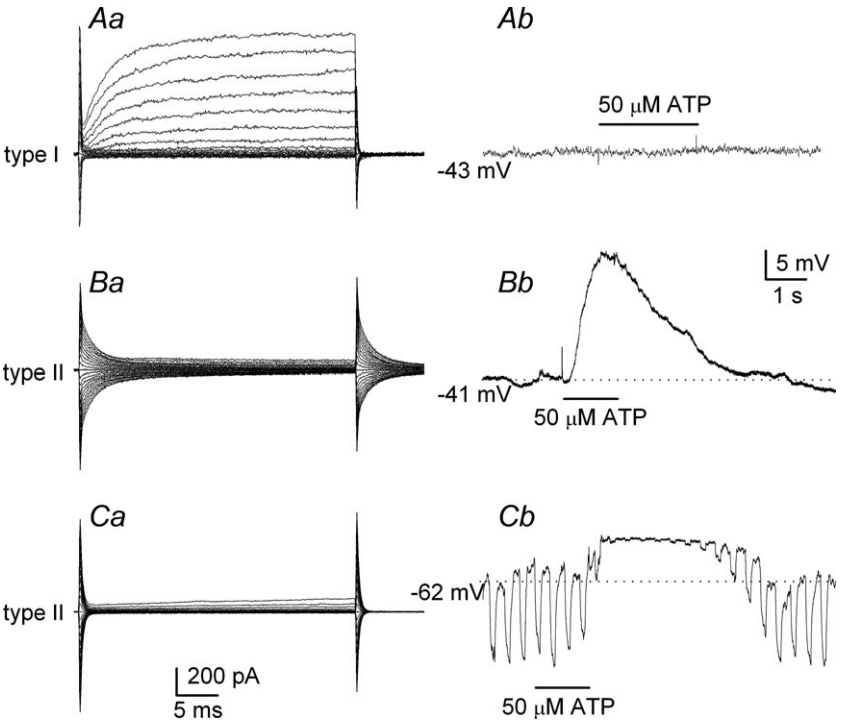


**Figure 2. Physiological profile of type I *versus* type II cells in chemoreceptor clusters, and the effect of ATP on membrane potential**
*Aa*, a voltage clamp recording showing typical, large voltage-activated outward $K^+$ currents in a type I cell, during steps from −60 mV (holding) to +60 mV; under current clamp, 50 $\mu$M ATP had no effect on membrane potential in the same cell (*Ab*). By contrast, under voltage clamp, type II cells typically show negligible (*Ba*) or small (*Ca*) voltage-activated outward currents and most show large capacitative transients as in *Ba*. Also, following ATP application, the same type II cells showed membrane depolarization after varying delays in *Bb* and *Cb*, respectively. Note, the depolarization was maintained for several seconds after the stimulus was terminated in *Bb* and *Cb*; it was associated with a significant increase in membrane conductance, as revealed by the injection of constant hyperpolarizing current pulses (*Cb*).

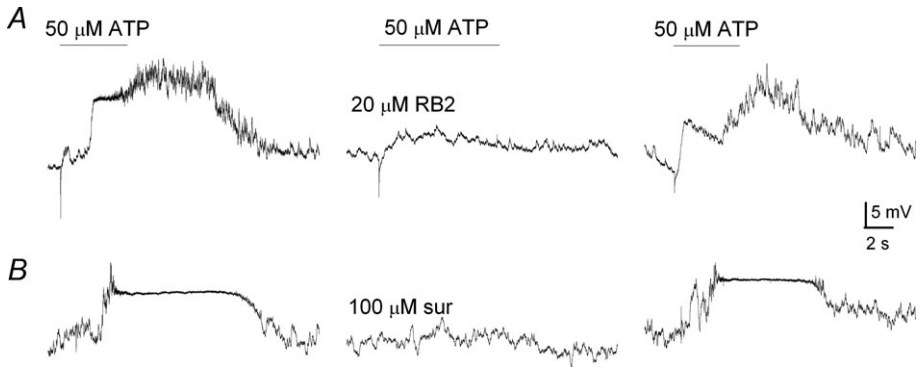


**Figure 3. Effects of purinergic P2 blockers on ATP-induced membrane depolarization in type II cells within glomus cell clusters (GCs)**
Exemplar traces showing the reversible inhibition of ATP-induced depolarization by the P2 receptor blockers, reactive blue 2 (RB2, 20 $\mu$M; upper traces) and suramin (100 $\mu$M; lower traces). Note the complex and prolonged variations in membrane potential after wash-out of ATP (50 $\mu$M) in both examples.

examined within GCs (see above), and it decreased with increasing ATP concentrations (Fig. 4*C*). Under these conditions, the minimum response latency was ~6 s and was reached at ATP concentrations ≥100 $\mu$M ($n = 5$).

## Reversal potential of ATP-induced currents in type II cells

When activated, pannexin channels behave as large conductance pores permeable to ions and large molecules

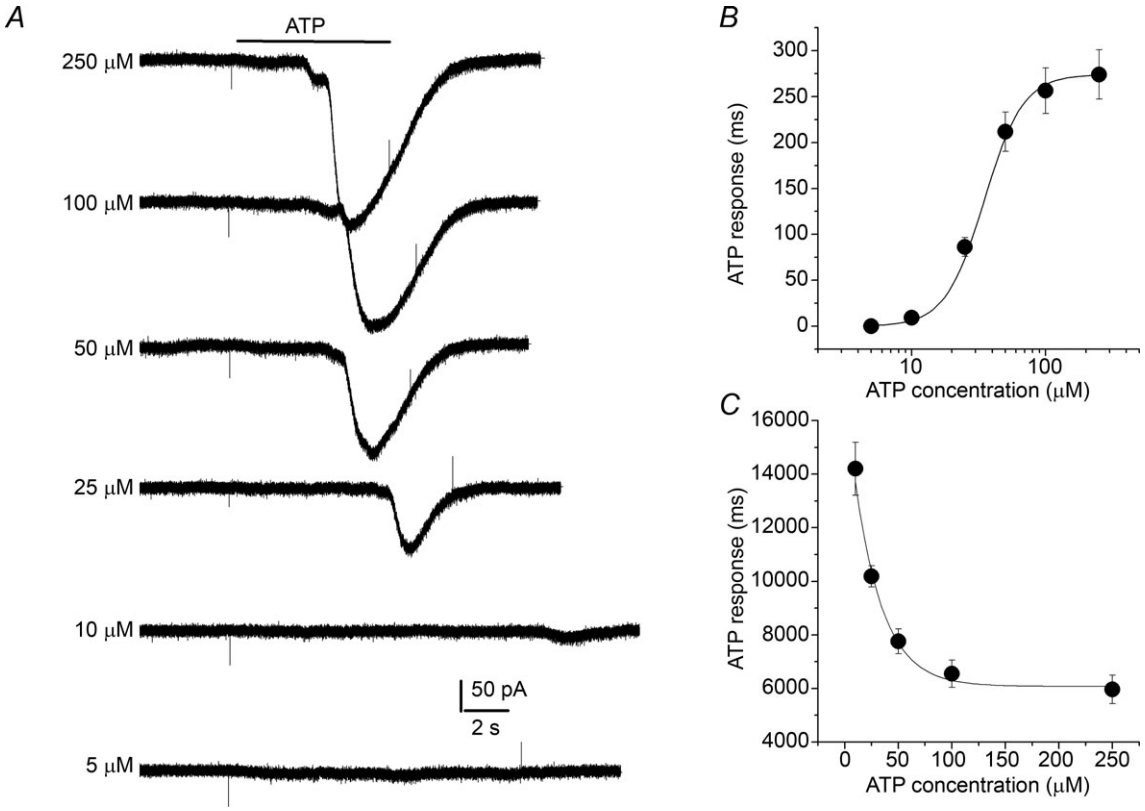


**Figure 4. Dose–response relationship and latency of ATP-activated currents in solitary type II cells located near glomus cell clusters**
*A*, exemplar whole-cell currents recorded from a solitary type II cell at a holding potential of −60 mV, following exposure to varying doses of ATP as indicated; note the increased latency of the current response as ATP concentration is decreased. *B*, the ATP dose–response curve fitted with the Hill equation ($EC_{50} = 34$ $\mu$M); data points indicate mean ± SEM ($n = 5$). *C*, curve shows mean (± SEM; $n = 5$) ATP response latency as a function of ATP concentration.

(Iglesias *et al.* 2009; MacVicar & Thompson, 2010). If ATP opens pannexin-1 non-selective ion channels in type II cells, then the ATP-activated currents should show a reversal potential characteristic of such channels (Bao *et al.* 2004; Locovei *et al.* 2006*b*; Ma *et al.* 2009). This was indeed the case as illustrated in Fig. 5*A* and *B* for a group of type II cells exposed to 50 $\mu$M ATP ($n = 5$). The mean reversal potential was ~0 mV, and the *I–V* curve showed a mild outward rectification and a mean slope conductance of ~4.2 nS at −50 mV, i.e. near the resting potential. Assuming a single channel conductance of ~500 pS (Bao *et al.* 2004; Thompson & Macvicar, 2008), this corresponds to the opening of approximately eight Panx-1 channels in type II cells exposed to 50 $\mu$M ATP.

## Sensitivity of ATP-induced inward currents to pannexin-1 blockers in type II cells

The pharmacological properties of Panx-1 channels closely resemble those of gap junctional proteins, making it difficult to distinguish one from the other. However, unlike gap junctions, pannexin-1channels are inhibited by low concentrations of carbenoxolone (CBX) and the stilbene derivative, 4,4′-diisothiocyano-2,2′-stilbenedisulfonic acid or DIDS (Bruzzone *et al.* 2005; Barbe *et al.* 2006; Huang *et al.* 2007*b*; Ma *et al.* 2009). As illustrated in Fig. 6*A* and *B*, the ATP-induced inward current (at −60 mV holding potential) was reversibly inhibited by 5 $\mu$M CBX ($n = 5$) and 10 $\mu$M DIDS ($n = 5$). In both cases the blockade developed slowly over a period of ~90 s (Fig. 6*C*), and was accompanied by a progressive increase in the latency of the ATP-induced current response (Fig. 6*D*). As expected for Panx-1 channels (Ma *et al.* 2009), the sensitivity of the ATP-induced inward current appeared higher for CBX compared to DIDS; whereas inhibition by 5 $\mu$M CBX was almost complete after 90 s exposure (Fig. 6*A*, middle traces; 6*C*), a residual current response was usually still detectable after exposure to DIDS at twice the concentration (Fig. 6*B*, middle traces and Fig. 6*C*). Taken together, this pharmacological profile is consistent with the opening of Panx-1 channels following exposure of type II cells to ATP.

## Purinergic activation of pannexin-1 channels in type II cells is mediated via P2Y2 receptors

Previous ratiometric $Ca^{2+}$ imaging and immunofluorescence studies demonstrated that type II cells of the rat CB express P2Y2Rs (Xu *et al.* 2003; Piskuric & Nurse, 2012), which, arguably, may couple to Panx-1 channels via increases in cytosolic $Ca^{2+}$ (Locovei *et al.* 2006*b*; Ma *et al.* 2009; MacVicar & Thompson, 2010). To test whether the delayed opening of Panx-1 channels following exposure of type II cells to ATP was attributable to activation of G-protein coupled P2Y2Rs, we used the agonist UTP, which displays roughly equal sensitivity at P2Y2 receptors as ATP (von Kugelgen, 2006). As illustrated in Fig. 7*A*, UTP (50 $\mu$M) activated an inward current with similar potency to that of ATP when applied to the same type II cell. The dose–response relation for UTP-evoked currents

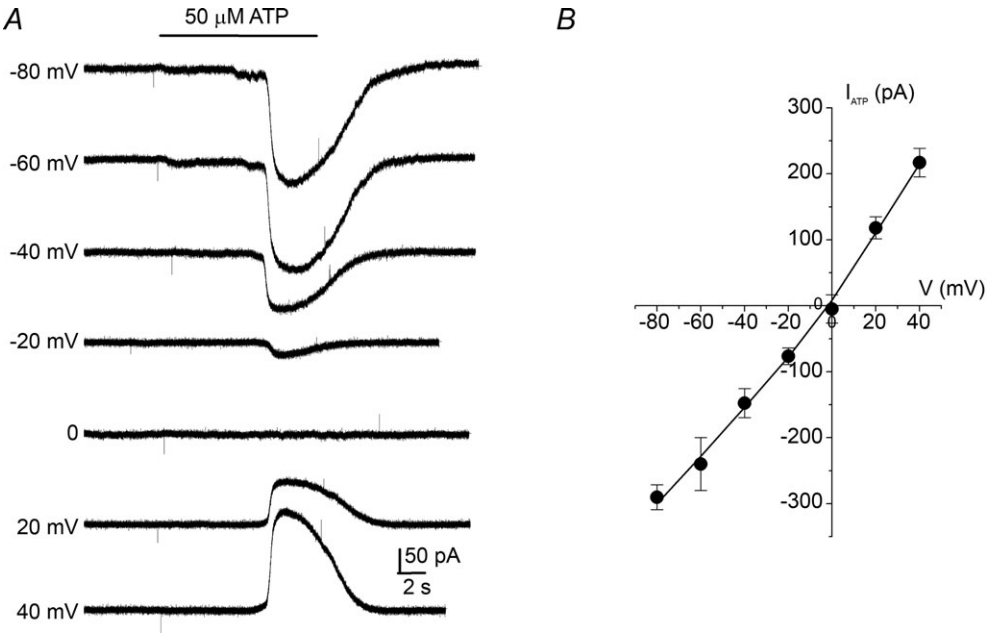


**Figure 5. Reversal potential of ATP-activated currents in type II cells**
*A*, exemplar traces of whole-cell currents evoked by 50 $\mu$M ATP at different membrane potentials. *B*, current–voltage (*I–V*) plot of ATP-evoked currents for a group of 5 type II cells showing a mean reversal potential at 0 mV, consistent with the opening of non-selective ion channels.

(at −60 mV holding potential) in a group of type II cells yielded an $EC_{50}$ of ∼37 $\mu$M (Fig. 7*B*; $n = 4$), similar to that for ATP ($EC_{50}$ ∼34 $\mu$M; Fig. 4*B*). In fact, the dose–response curves for ATP and UTP were practically superimposable (Fig. 7*B*), as expected for P2Y2Rs. The reversal potential for UTP-evoked currents was also approximately 0 mV ($n = 2$; data not shown), as demonstrated for ATP (Fig. 5), and consistent with the opening of non-selective ion channels.

We also used ratiometric $Ca^{2+}$ imaging to confirm the selective expression of P2Y2Rs on type II cells. As previously demonstrated in more detailed studies on dissociated rat CB cells (Xu *et al.* 2003; Piskuric & Nurse, 2012), both UTP and ATP (100 $\mu$M) evoked similar increases in intracellular $Ca^{2+}$ in type II cells (e.g. Fig. 7*C*; lower traces). However, consistent with previous reports (Xu *et al.* 2003, 2005), neither purine at this concentration evoked a detectable $Ca^{2+}$ response in a nearby type I cell in the same culture (Fig. 7*C*; upper trace); note positive identification of the type I cell by a large $[\Delta Ca^{2+}]_i$ response to hypercapnia (10% $CO_2$) and the depolarizing stimulus high $K^+$ (30 mM), both of which fail to affect the type II cells (Fig. 7*C*; lower traces). The mean $\Delta[Ca^{2+}]_i$ evoked by 100 $\mu$M ATP and UTP in type I cells was $1.0 \pm 4.6$ nM and $-2.4 \pm 4.4$ nM ($n = 50$); a small $Ca^{2+}$ signal of unknown origin was sometimes detected in type I cells after washout of ATP and UTP (e.g. Fig. 7*C*; upper trace). By contrast, the depolarizing stimulus (high $K^+$) evoked large increases in cytosolic $Ca^{2+}$ in purine-insensitive type I cells (mean $\Delta[Ca^{2+}]_i = 226.5 \pm 20.0$ nM; $n = 50$).

## Evidence for ATP release via Panx-1 channels from type II cells following P2Y2 receptor activation

It is well documented that opening of Panx-1 channels leads to ATP release from a variety of cell types including

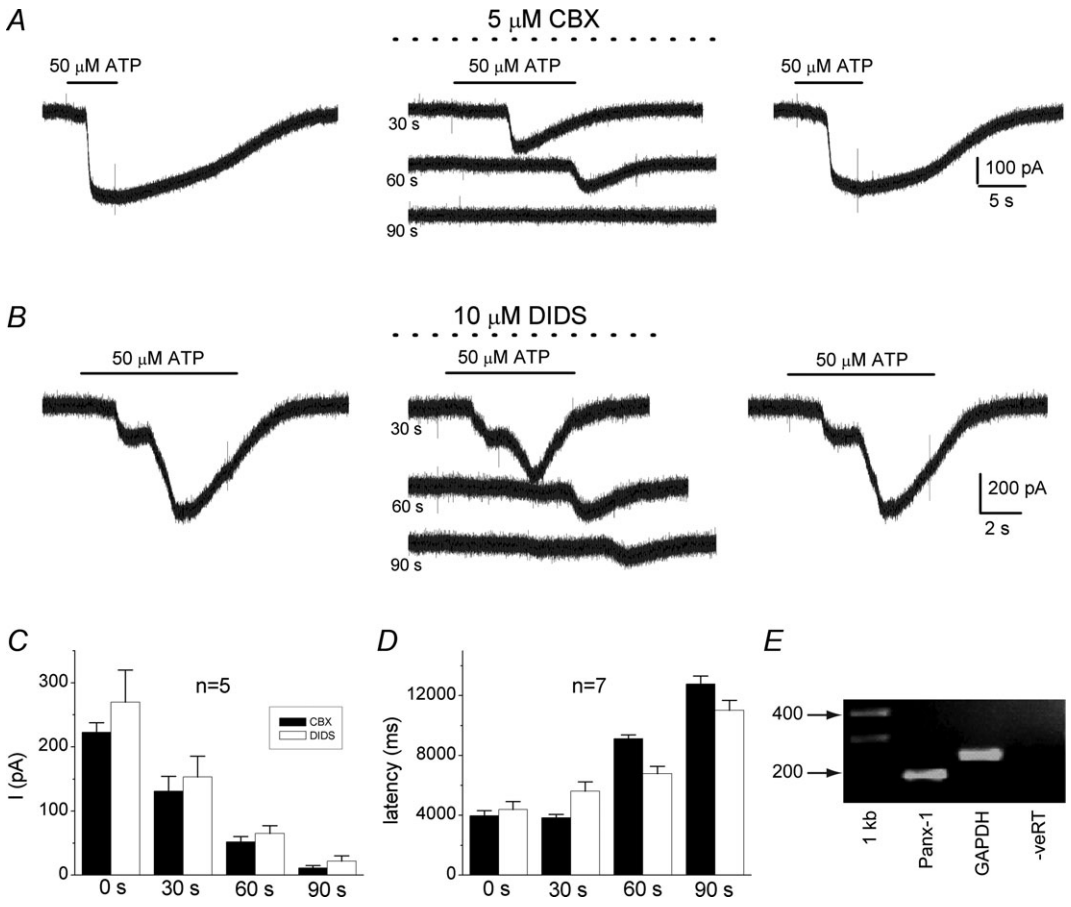


**Figure 6. Effects of pharmacological blockers of Panx-1 channels on ATP-induced whole-cell currents in type II cells and expression of Panx-1 mRNA in whole rat carotid bodies**
The selective Panx-1 inhibitors carbenoxolone (CBX; 5 $\mu$M) and DIDS (10 $\mu$M) caused a slowly developing blockade of the inward current induced by 50 $\mu$M ATP (at −60 mV holding potential) in *A* and *B* respectively. Note blockade was readily reversible and developed gradually over a period of 90 s, in parallel with an increase in latency of the residual response. Histograms of the time-dependent inhibition of the inward current and the increase in response latency are shown in *C* and *D* respectively; data are represented as means ± SEM. *E*, gel showing expression of Panx-1 mRNA in extracts of whole rat carotid bodies.

erythrocytes and brain astrocytes (Locovei *et al.* 2006*a*; Huang *et al.* 2007*a*; Iglesias *et al.* 2009; MacVicar & Thompson, 2010; Sridharan *et al.* 2010). Given that ATP is a key excitatory neurotransmitter released from type I cells during chemoexcitation (Nurse, 2010), we wondered whether autocrine P2Y2R activation in type II cells among (or close to) GCs could lead to signal amplification via ATP-induced ATP release. To this end we used a co-culture model of the CB consisting of GCs and juxtaposed dissociated afferent (petrosal) neurones (Zhong *et al.* 1997, 2000). This model contains all the elements of the tripartite complex in close proximity, i.e. receptor type I cells, glia-like type II cells, and sensory petrosal neurones (PNs), and was previously used to demonstrate co-release of ACh and ATP from presynaptic type I cells onto postsynaptic PNs during chemotransduction (Zhang *et al.* 2000; Zhang & Nurse, 2004; Nurse, 2010). Because these PNs express predominantly ligand-gated P2X2/3 purinoceptors (Prasad *et al.* 2001), the goal here was to use juxtaposed PNs (within the tripartite complex) as sensitive reporters of ATP release from type II cells.

To selectively activate type II cells and cause opening of Panx-1 channels, we used the agonist UTP (50 $\mu$M) which at this concentration has no direct effect on either type I cells (Xu *et al.* 2005) (see also Fig. 7*C*), or P2X-expressing PNs (see below). However, given the inherent limitations of this preparation imposed by the monolayer conditions, lack of specialized contacts between type II cells and PNs, infrequency of type II cells within GCs, and the fast perfusion rate, successful cases were expected to be rare. Indeed, in perforated-patch recordings from >60 juxtaposed PNs, we found seven cases where rapid application of UTP over the tripartite complex led to PN depolarization or action potential firing (Figs 8 and 9*A* and *B*), consistent with ATP release from type II cells. In one successful case (Fig. 8), we were fortunate in first obtaining stable, simultaneous, dual recordings from a

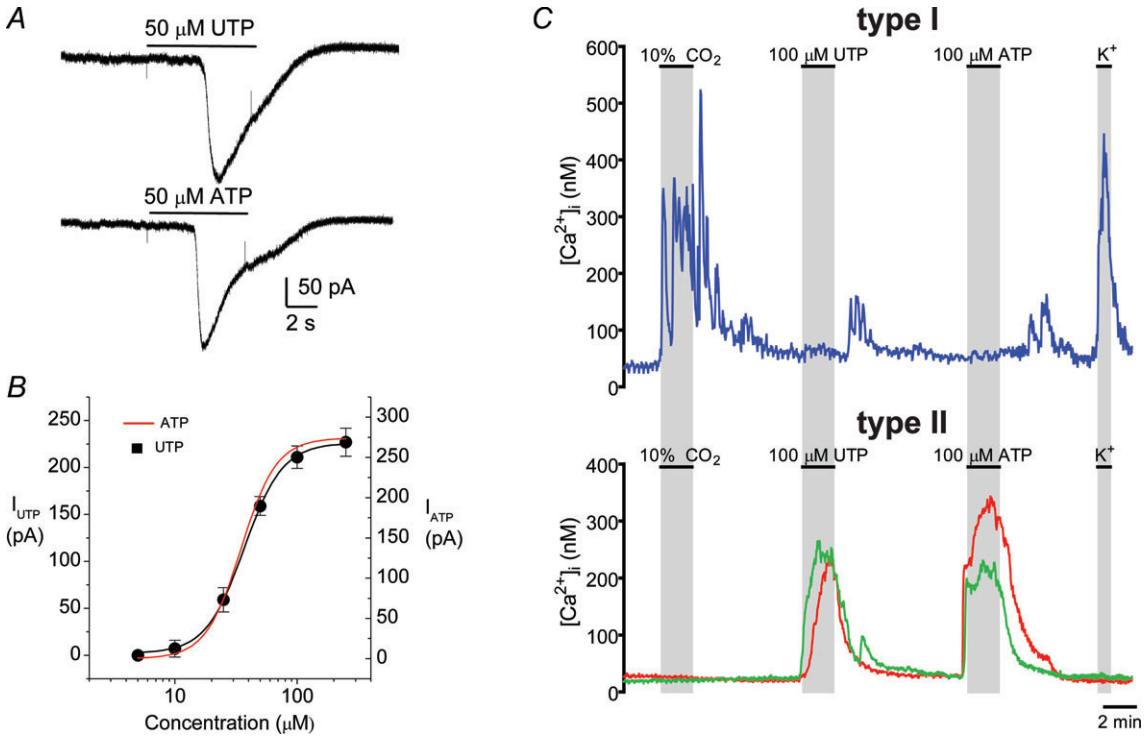


**Figure 7. Purinergic activation of Panx-1-like currents in type II cells is mediated by P2Y2 receptors in association with a rise in intracellular $Ca^{2+}$**
*A*, both ATP and UTP (50 $\mu$M) induce inward currents (at −60 mV) of similar magnitude in the *same* type II cell as expected for P2Y2 receptors. *B*, dose–response relation for the UTP-evoked currents in a group of type II cells is shown by the black curve; data are represented as means ± SEM ($n = 4$) and fitted with the Hill equation with an $EC_{50} = 37$ $\mu$M. The dose–response curve for ATP (red) from Fig. 4*B* is superimposed and is indistinguishable from that for UTP. *C*, intracellular $Ca^{2+}$ responses monitored simultaneously in type I and type II cells located in different regions of the same culture. Note that both hypercapnia (10% $CO_2$) and the depolarizing stimulus high (30 mM) $K^+$ induce robust $\Delta[Ca^{2+}]_i$ responses in the type I cell (upper trace), but are ineffective in the two type II cells (lower traces). Conversely, ATP and UTP induced comparable robust $\Delta[Ca^{2+}]_i$ responses in both type II cells, but not in the type I cell; small $Ca^{2+}$ responses of unknown origin were sometimes seen in the type I cell *after* removal of each purine (upper trace). Period during which each stimulus was applied is indicated by the shaded vertical bars.

PN and a nearby type II cell under voltage clamp (Fig. 8, upper traces). After switching to current clamp (Fig. 8; left and right lower 3 traces), perfusion of 50 $\mu$M UTP led to depolarization in both cells that was reversibly inhibited by 5 $\mu$M CBX (Fig. 8; lower middle traces); the greater delay in the type II cell response after UTP application, compared to that of the PN, suggests that other type II cell(s) within the juxtaposed GC cluster initiated the PN response. Nonetheless, the data suggested a link between PN depolarization and opening of CBX-sensitive Panx-1 channels. In the remaining six successful cases (e.g. Fig. 9*A* and *B*), a single electrode was used to record the excitatory response in the juxtaposed PN following UTP application to the tripartite complex. For PNs where recordings remained stable over the duration of the experiment, which sometimes included drug perfusions (see below), the mean depolarization induced by UTP was $3.8 \pm 0.9$ mV ($n = 4$). These data are consistent with the idea that Panx-1 channel opening in nearby type II cell(s) caused ATP to be released onto the recorded PN.

To demonstrate directly that ATP release from type II cells was the cause of the PN depolarization we used the P2X2/3 receptor blocker, pyridoxalphosphate-6-azophenyl-2′,4′-disulphonic acid (PPADS; 10 $\mu$M). As exemplified in Fig. 9 ($n = 4$), the UTP-induced depolarization (Fig. 9*A*) and/or spike activity (Fig. 9*B*) in juxtaposed PNs were reversibly inhibited by PPADS (Fig. 9*A* and *B*; middle traces), confirming their dependence on ATP release from type II cells. It should be noted that at the concentration 10 $\mu$M, PPADS had no effect on the UTP-induced inward

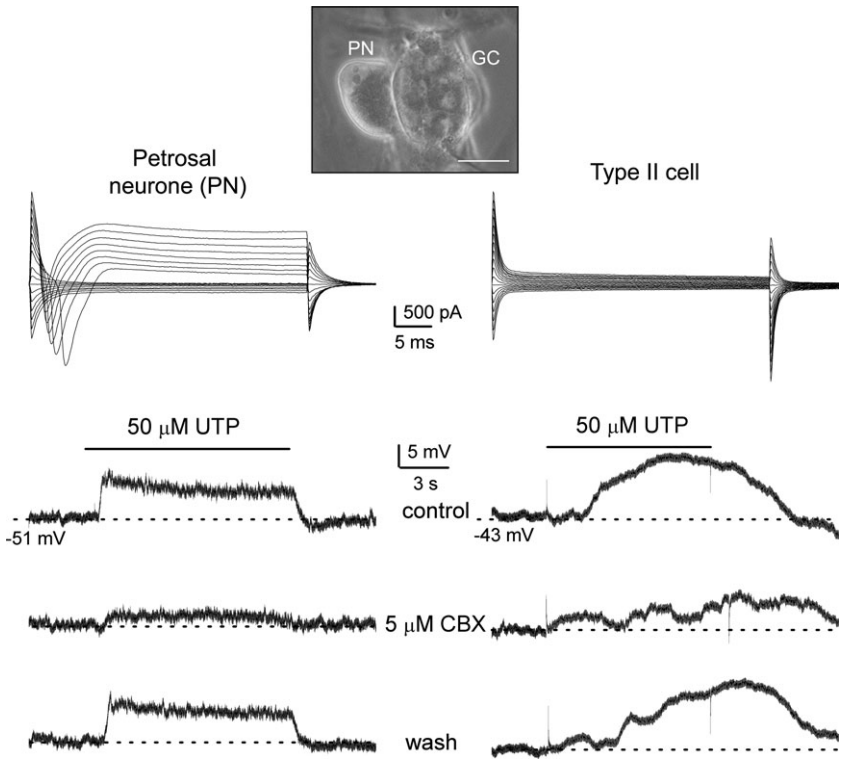


**Figure 8. Involvement of Panx-1 channels in UTP-induced depolarization in a type II cell and nearby petrosal neurone in carotid body co-culture**
Top, example of a phase contrast micrograph showing a glomus/type II cell cluster (GC) and juxtaposed petrosal neurone (PN) as a tripartite complex (scale bar = 20 $\mu$m); this configuration was used in assays for ATP release from type II cells via Panx-1 channels, where P2X2/3 receptors on the PN served as a reporter or biosensor of ATP release (see Fig. 9). Simultaneous paired recordings from a PN and a type II cell (near a GC cluster) are shown in left and right columns, respectively. Upper traces are voltage clamp recordings showing typical whole-cell currents from the PN (left) and type II cell (right); note voltage-gated inward and outward currents in the PN during depolarizing voltage steps from −60 mV (holding potential). Application of 50 $\mu$M UTP (lower 3 traces in each column) induced membrane depolarization in both PN and type II cell that was reversibly inhibited by the Panx-1 blocker, carbenoxolone (CBX, 5 $\mu$M; middle traces). As UTP fails to activate P2X2/3 receptors on PN directly, the UTP-evoked responses seen in the PN were indirect, i.e. secondary to Panx-1 channel opening in type II cells. The longer latency of the UTP response in the type II cell (relative to the PN) implies that other type II cell(s) contributed to the initiation of the PN response.

currents in type II cells (Fig. 9*D* and *F*), as expected from its known relative insensitivity at P2Y2Rs (von Kugelgen, 2006). Also in Fig. 9*C* and *E*, we confirmed that 10 $\mu$M PPADS almost completely abolished the inward current induced by 5 $\mu$M ATP applied to the soma of isolated PNs; this ATP concentration is $\sim$2$\times$ the $EC_{50}$ for ATP at the P2X2/3 receptors expressed on these neurones ($EC_{50} = 2.7$ $\mu$M; Zhang *et al.* 2000).

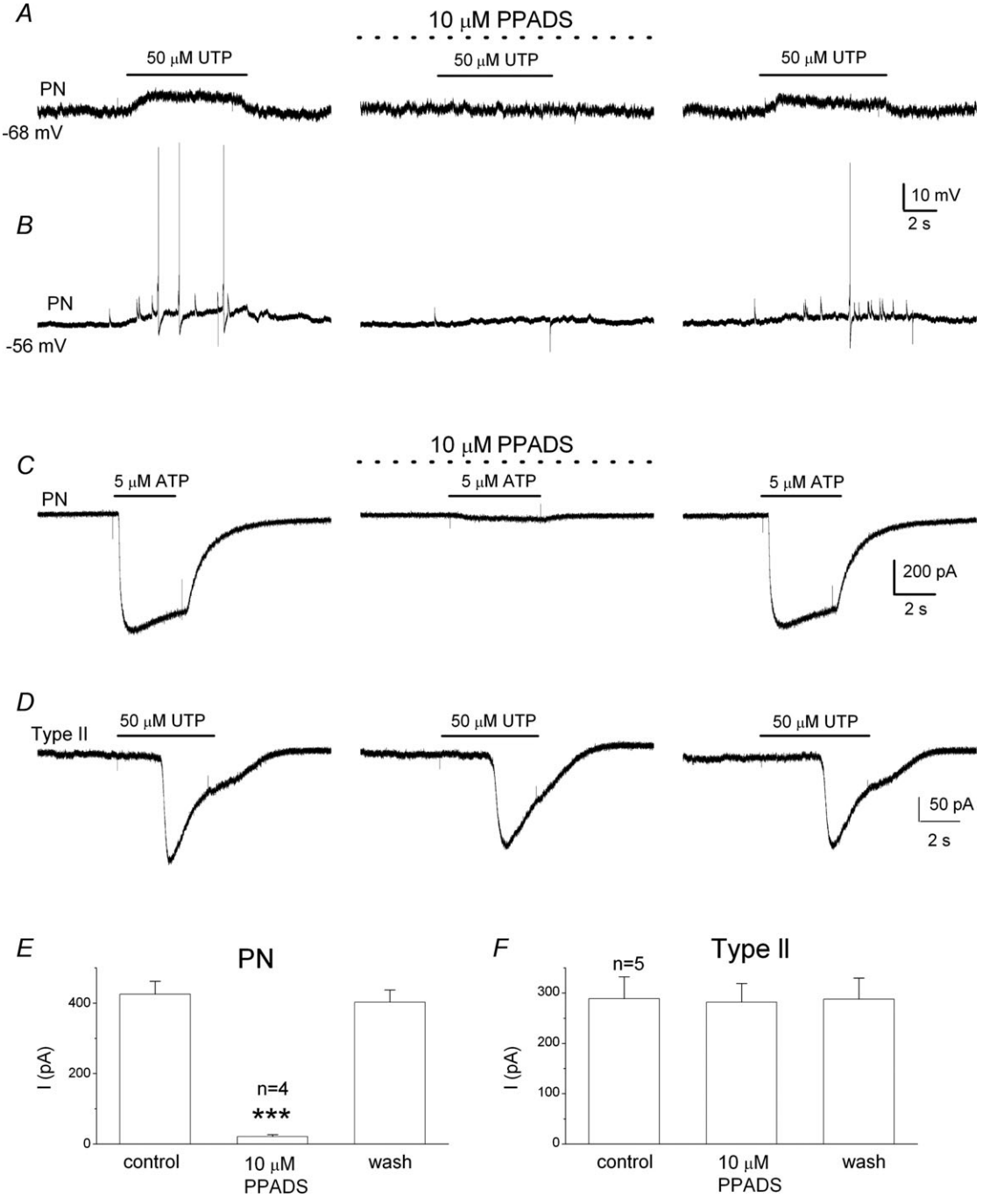


**Figure 9. Evidence for ATP release from type II cells following activation of P2Y2 receptors using petrosal neurones as ATP biosensors**
Using the co-culture configuration described in Fig. 8, application of UTP over the tripartite complex evoked depolarization (*A*) or action potential firing (*B*) in the juxtaposed PNs. In both cases the response was reversibly abolished during perfusion of the P2X2/3 receptor blocker PPADS (10 $\mu$M; middle traces), consistent with release of ATP. Note that 10 $\mu$M PPADS almost completely abolishes ATP-evoked currents in isolated PNs (*C* and *E*; for *E*, $^{***}P < 0.001$, ANOVA), but fails to affect UTP-induced whole-cell currents in type II cells (*D* and *F*; for *F*, $P > 0.05$, ANOVA).

## Discussion

The present study has uncovered a potentially novel role for type II cells in carotid body (CB) function. These cells, variously described as glia-like, sheath, or sustentacular cells (McDonald & Mitchell, 1975; Kondo, 2002), have long been known to form intimate associations with chemoreceptor type I cells, but there has been no direct evidence that they may actively participate in the transmission of sensory signals to the afferent nerve terminal. In the present study, we demonstrate for the first time that the gap junction-like proteins, i.e. pannexin-1 (Panx-1) channels, are expressed in type II cells and that they form conduits for ATP release, when opened following activation of G-protein coupled P2Y2 receptors (P2Y2Rs) on these cells. Given that ATP is a key excitatory neurotransmitter released from type I cells during chemotransduction (Nurse, 2010), our model proposes that as a result of the paracrine action of ATP, type II cells could further amplify the ATP signal and therefore contribute to chemoexcitation via the mechanism of ATP-induced ATP release, as illustrated in Fig. 10. Strong support for this model was obtained in co-culture experiments where chemoafferent petrosal neurones were grown together with chemoreceptor cell clusters, containing both type I and type II cells. We demonstrated that within this tripartite complex selective activation of P2Y2Rs on type II cells with UTP caused a delayed release of ATP via Panx-1 channels, leading to depolarization/excitation of juxtaposed P2X-expressing petrosal neurones. Interestingly, in another chemosensory organ, i.e. the taste bud, gustatory stimuli have been shown to induce ATP release from receptor cells via Panx-1 channels (Huang *et al.* 2007*b*).

### Physiological activation of Panx-1 channels in type II cells

Our interest in type II cells as likely participants in sensory signalling in the CB was heightened with the immunocytochemical demonstration that these cells express Panx-1 channels, and that Panx-1 mRNA was expressed in whole CB extracts. Confocal immunofluorescence studies on CB tissue sections revealed that Panx-1 was localized to the soma and processes of type II cells, which closely enveloped TH-positive, but Panx1-negative, type I cells. Further, in dissociated CB cultures Panx-1 and TH labelled separate and distinct cell populations, and Panx-1 labelling co-localized with that of GFAP, an established marker for type II cells (Nurse & Fearon, 2002; Pardal *et al.* 2007). Because P2Y2Rs were previously known to be expressed in type II cells (Xu *et al.* 2003), and activation of Panx-1 channels by ATP has been proposed to occur via P2YRs and elevations in cytoplasmic $Ca^{2+}$ (Locovei *et al.* 2006*b*), we hypothesized that activation of P2Y2Rs on type II cells may lead to Panx-1 channel opening. Consistent with this view, we found that the P2Y2R agonists ATP and UTP

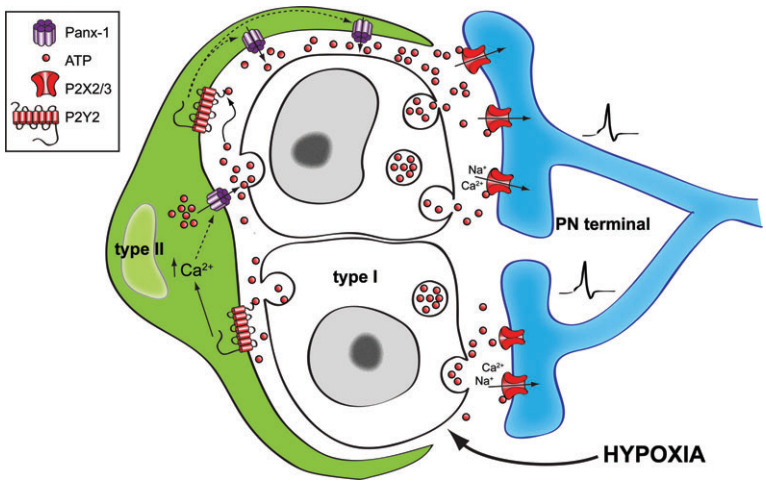


**Figure 10. Model of the carotid body tripartite synapse**
It is proposed that during hypoxia ATP is released from chemoreceptor type I cells, leading to direct excitation of petrosal afferent terminals via P2X2/3Rs. Additionally, this released ATP can cause paracrine activation of P2Y2Rs on contiguous type II cells, leading to a rise in intracellular $Ca^{2+}$, opening of Panx-1 channels and release of ATP. This results in signal amplification via ATP-induced ATP release, and may be facilitated by the propagation of ATP waves involving the same or adjacent type II cells. For clarity details of termination or modification of the ATP signal are omitted but include (i) breakdown of ATP to adenosine by ecto-5′-nucleotidases (Conde & Monteiro, 2004), (ii) negative feedback closure of Panx-1 channels when extracellular ATP levels become too high (Dubyak, 2009), and (iii) negative feedback inhibition of chemoreceptor function via ATP acting at P2Y1Rs on type I cells (Xu *et al.* 2005).

caused a delayed opening of non-selective ion channels (reversal potential ∼0 mV) that led to a prolonged membrane depolarization. The latter often outlasted the duration of the stimulus, suggesting involvement of a G-protein coupled pathway, and sometimes displayed complex fluctuations in membrane potential that may be due to the multiple conductance states characteristic of Panx-1 channels (Bao *et al.* 2004; Locovei *et al.* 2006*b*; MacVicar & Thompson, 2010), or sequential opening of Panx-1 channels following ATP-induced ATP release. The observation that the response latency tended to be much shorter when type II cells were present within chemoreceptor cell clusters, compared to when present as solitary cells in isolation, might suggest a more effective coupling between P2Y2R and Panx-1 channels when type II cells are in their native cellular microenvironment, i.e. near contiguous type I cells (Kondo, 2002). This coupling is likely to be influenced by the spatial relationship between plasmalemmal P2Y2Rs, Panx-1 channels, and intracellular $Ca^{2+}$ stores, and this relationship might be perturbed in solitary, isolated type II cells. Importantly, the ATP-induced opening of the non-selective ion channels was reversibly inhibited by low concentrations of carbenoxolone (5 $\mu$M) and DIDS (10 $\mu$M), consistent with the pharmacology of Panx-1 channels (Bruzzone *et al.* 2005; Barbe *et al.* 2006; Huang *et al.* 2007*a*; Thompson & Macvicar, 2008; Ma *et al.* 2009; MacVicar & Thompson, 2010). Even though the possibility that type I and type II cells might be connected by gap junctions was once considered, but later refuted (Kondo, 2002), it is unlikely that the low concentration of carbenoxolone used in the present study was sufficient to block gap junctional hemichannels (Thompson & Macvicar, 2008), should they exist in type II cells. While the link between P2Y2R activation and opening of Panx-1 channels in type II cells is at present unclear, it is tempting to suggest that the rise in intracellular $Ca^{2+}$ was involved. In previous studies (Xu *et al.* 2003; Piskuric & Nurse, 2012), as well as the present one, the P2Y2R agonists ATP and UTP (100 $\mu$M) caused a rise in intracellular $Ca^{2+}$ in the range 0.3 to 1 $\mu$M in type II cells. Interestingly, in oocyte expression systems micromolar amounts of cytoplasmic $Ca^{2+}$ have been shown to open human Panx-1 channels in excised membrane patches (Locovei *et al.* 2006*b*), though regulation of these channels by $Ca^{2+}$ has been questioned in another study (Ma *et al.* 2009). Thus, elevation in intracellular $Ca^{2+}$ remains a potential link between P2Y2R stimulation and opening of Panx-1 channels in type II cells, though further studies are needed to clarify this pathway. Because Panx-1 channels behave as non-selective pores, it is plausible that extracellular $Ca^{2+}$ entry through these pores after the initial opening may contribute to the rise in intracellular $Ca^{2+}$ following P2Y2R activation in type II cells (Xu *et al.* 2003).

### P2Y2R-mediated opening of Panx-1 channels leads to ATP release from type II cells

Using a co-culture model of dissociated petrosal ganglion neurones (PNs) and glomus cell clusters (GCs) with contiguous type II cells, we found evidence for ATP release via Panx-1 channels, despite the non-ideal conditions inherent in this preparation. First, type II cells are 3–4 times less abundant than type I cells in the rat CB (McDonald & Mitchell, 1975), and represent a smaller fraction of the cells within cultured isolated GCs (Nurse & Fearon, 2002; Piskuric & Nurse, 2012). Second, the fast perfusion technique used for agonist stimulation of P2Y2Rs was likely to favour rapid diffusion of any released ATP away from the biosensor, i.e. the juxtaposed PN, whose terminals do not appear to form specialized contacts with type II cells (Kondo, 2002). Third, the assay required that the PN soma or processes be fortuitously positioned near sites of 'contact' with the type II cell, and that P2X2/3 receptors on the former be located close to Panx-1 channels on the latter. Despite these constraints, after many trials we obtained several successful cases where selective activation of P2Y2Rs on type II cells with the agonist UTP led to membrane depolarization or increased action potential firing in the soma of a juxtaposed PN. The latter case implied that within the tripartite complex, activation of type II cell(s) *alone* could, remarkably, cause excitation of the afferent neurone. The PN depolarization depended on Panx-1 channel opening because it could be inhibited by low concentrations of carbenoxolone, and involved ATP release, because it could be reversibly abolished by PPADS (10 $\mu$M). At this concentration PPADS was ineffective at P2Y2Rs on type II cells, but inhibited ligand-gated P2X2/3Rs on petrosal chemoafferent neurones, as expected from the known pharmacology of these receptors (von Kugelgen, 2006; Nurse, 2010). The use of UTP (50 $\mu$M) as the agonist ensured that only P2Y2Rs on type II cells were stimulated within the tripartite complex, as other P2 receptors, i.e. P2Y1Rs on type I cells and P2X2/3Rs on PNs are relatively insensitive to UTP (Xu *et al.* 2003, 2005). Taken together, these data indicate that stimulation of P2Y2Rs on type II cells could excite petrosal neurones via ATP release from open Panx-1 channels. Future experiments using more specific Panx-1 blockers are required to validate a role of these channels in CB physiology in more intact preparations. In this regard it is noteworthy that in the perfused–superfused cat CB *in vitro*, DIDS (10 $\mu$M), an anion transport blocker as well as a non-selective Panx-1 channel blocker, decreased the sinus nerve chemosensory baseline discharge, eliminated the initial peak responses to hypoxia and hypercapnia, and increased the time to achieve the maximal response (Iturriaga *et al.* 1998). Though the latter effects were presumed to be mediated via anion channel blockade, in light of the

present study the possibility is raised that Panx-1 channel block by DIDS may have been a contributing factor (see Fig. 6*B*).

### Significance of findings to carotid body function

The data presented here suggest a novel mechanism by which type II cells could actively participate in signal processing in the mammalian CB during chemoexcitation. As summarized in Fig. 10, the model proposes that during chemotransduction by stimuli such as hypoxia, receptor type I cells release ATP (among other excitatory transmitters and modulators), which acts on post-synaptic P2X2/3 purinoceptors on petrosal chemoafferent terminals causing excitation (Nurse, 2010). Released ATP can also have paracrine functions which include the activation of P2Y2Rs on contiguous type II cells, leading to the opening of Panx-1 channels located on the soma and/or along the spindle-like processes of these cells. Panx-1 channels serve as conduits for ATP release from type II cells, which could lead to further activation of P2Y2Rs and opening of Panx-1 channels, thereby enhancing the extracellular ATP pool in the vicinity of the afferent nerve terminal. In this way, type II cells can be seen as active contributors to the resulting sensory discharge by acting as ATP amplifiers. Given the type II cell morphology, with its elongated, spindle-shaped processes that ensheath the chemoreceptor clusters, it is plausible that ATP released from a type II cell could act on P2Y2Rs on the same or adjacent cells, causing opening of Panx-1 channels, and ultimately leading to the propagation of ATP waves. High levels of extracellular ATP can lead to closure of Panx-1 channels (Dubyak, 2009), providing a negative feedback pathway which could help prevent excessive loss of ATP and other key cellular contents from type II cells. Also during hypoxia, extracellular ATP could act in an autocrine–paracrine manner at P2Y1Rs on type I cells to cause hyperpolarization, and limit secretion of ATP by a negative feedback mechanism (Xu *et al.* 2005). Additionally, the presence of ectonucleotidases can help terminate the action of extracellular ATP at the sensory synapse, in part by converting it to adenosine, another key CB excitatory neuromodulator (Conde & Monteiro, 2004; Nurse, 2010; Conde *et al.* 2012). In conclusion, we propose that the type II cell may take part in the process of 'gliotransmission' in the CB by acting as an ATP amplifier; this is mediated by a mechanism of ATP-induced ATP release involving P2Y2Rs and Panx-1 channels. It therefore adds to a growing list, amply demonstrated in the central nervous system (Eroglu & Barres, 2010; MacVicar & Thompson, 2010; Parpura *et al.* 2012), where glial cells play a prominent role in synaptic integration and connectivity at tripartite synapses.

## References


Bao L, Locovei S & Dahl G (2004). Pannexin membrane channels are mechanosensitive conduits for ATP. *FEBS Lett* **572**, 65–68.

Barbe MT, Monyer H & Bruzzone R (2006). Cell-cell communication beyond connexins: the pannexin channels. *Physiology (Bethesda)* **21**, 103–114.

Bruzzone R, Barbe MT, Jakob NJ & Monyer H (2005). Pharmacological properties of homomeric and heteromeric pannexin hemichannels expressed in *Xenopus* oocytes. *J Neurochem* **92**, 1033–1043.

Campanucci VA, Dookhoo L, Vollmer C & Nurse CA (2012). Modulation of the carotid body sensory discharge by NO: An up-dated hypothesis. *Respir Physiol Neurobiol* (in press).

Campanucci VA, Zhang M, Vollmer C & Nurse CA (2006). Expression of multiple P2X receptors by glossopharyngeal neurons projecting to rat carotid body $O_2$-chemoreceptors: role in nitric oxide-mediated efferent inhibition. *J Neurosci* **26**, 9482–9493.

Conde SV & Monteiro EC (2004). Hypoxia induces adenosine release from the rat carotid body. *J Neurochem* **89**, 1148–1156.

Conde SV, Monteiro EC, Rigual R, Obeso A & Gonzalez C (2012). Hypoxic intensity: a determinant for the contribution of ATP and adenosine to the genesis of carotid body chemosensory activity. *J Appl Physiol* **112**, 2002–2010.

Drummond GB (2009). Reporting ethical matters in *The Journal of Physiology*: standards and advice. *J Physiol* **587**, 713–719.

Dubyak GR (2009). Both sides now: multiple interactions of ATP with pannexin-1 hemichannels. Focus on "A permeant regulating its permeation pore: inhibition of pannexin 1 channels by ATP". *Am J Physiol Cell Physiol* **296**, C235–241.

Duchen MR, Caddy KW, Kirby GC, Patterson DL, Ponte J & Biscoe TJ (1988). Biophysical studies of the cellular elements of the rabbit carotid body. *Neuroscience* **26**, 291–311.

Eroglu C & Barres BA (2010). Regulation of synaptic connectivity by glia. *Nature* **468**, 223–231.

Eyzaguirre C & Zapata P (1984). Perspectives in carotid body research. *J Appl Physiol* **57**, 931–957.

Gonzalez C, Almaraz L, Obeso A & Rigual R (1994). Carotid body chemoreceptors: from natural stimuli to sensory discharges. *Physiol Rev* **74**, 829–898.

Huang Y, Grinspan JB, Abrams CK & Scherer SS (2007*a*). Pannexin1 is expressed by neurons and glia but does not form functional gap junctions. *Glia* **55**, 46–56.

Huang YJ, Maruyama Y, Dvoryanchikov G, Pereira E, Chaudhari N & Roper SD (2007*b*). The role of pannexin 1 hemichannels in ATP release and cell-cell communication in mouse taste buds. *Proc Natl Acad Sci USA* **104**, 6436–6441.

Iglesias R, Dahl G, Qiu F, Spray DC & Scemes E (2009). Pannexin 1: the molecular substrate of astrocyte "hemichannels". *J Neurosci* **29**, 7092–7097.

Iturriaga R & Alcayaga J (2004). Neurotransmission in the carotid body: transmitters and modulators between glomus cells and petrosal ganglion nerve terminals. *Brain Res Brain Res Rev* **47**, 46–53.

Iturriaga R, Mokashi A & Lahiri S (1998). Anion exchanger and chloride channel in cat carotid body chemotransduction. *J Auton Nerv Syst* **70**, 23–31.

Kondo H (2002). Are there gap junctions between chief (glomus, type I) cells in the carotid body chemoreceptor? A review. *Microsc Res Tech* **59**, 227–233.

Lai CP, Bechberger JF, Thompson RJ, MacVicar BA, Bruzzone R & Naus CC (2007). Tumor-suppressive effects of pannexin 1 in C6 glioma cells. *Cancer Res* **67**, 1545–1554.

Locovei S, Bao L & Dahl G (2006*a*). Pannexin 1 in erythrocytes: function without a gap. *Proc Natl Acad Sci USA* **103**, 7655–7659.

Locovei S, Wang J & Dahl G (2006*b*). Activation of pannexin 1 channels by ATP through P2Y receptors and by cytoplasmic calcium. *FEBS Lett* **580**, 239–244.

Ma W, Hui H, Pelegrin P & Surprenant A (2009). Pharmacological characterization of pannexin-1 currents expressed in mammalian cells. *J Pharmacol Exp Ther* **328**, 409–418.

McDonald DM & Mitchell RA (1975). The innervation of glomus cells, ganglion cells and blood vessels in the rat carotid body: a quantitative ultrastructural analysis. *J Neurocytol* **4**, 177–230.

MacVicar BA & Thompson RJ (2010). Non-junction functions of pannexin-1 channels. *Trends Neurosci* **33**, 93–102.

Nurse CA (2005). Neurotransmission and neuromodulation in the chemosensory carotid body. *Auton Neurosci* **120**, 1–9.

Nurse CA (2010). Neurotransmitter and neuromodulatory mechanisms at peripheral arterial chemoreceptors. *Exp Physiol* **95**, 657–667.

Nurse CA & Fearon IM (2002). Carotid body chemoreceptors in dissociated cell culture. *Microsc Res Tech* **59**, 249–255.

Pardal R, Ortega-Saenz P, Duran R & Lopez-Barneo J (2007). Glia-like stem cells sustain physiologic neurogenesis in the adult mammalian carotid body. *Cell* **131**, 364–377.

Parpura V, Heneka MT, Montana V, Oliet SH, Schousboe A, Haydon PG, Stout RF Jr, Spray DC, Reichenbach A, Pannicke T, Pekny M, Pekna M, Zorec R & Verkhratsky A (2012). Glial cells in (patho)physiology. *J Neurochem* **121**, 4–27.

Piskuric NA & Nurse CA (2012). Effects of chemostimuli on $[Ca^{2+}]_i$ responses of rat aortic body type I cells and endogenous local neurons: comparison with carotid body cells. *J Physiol* **590**, 2121–2135.

Prasad M, Fearon IM, Zhang M, Laing M, Vollmer C & Nurse CA (2001). Expression of P2X2 and P2X3 receptor subunits in rat carotid body afferent neurones: role in chemosensory signalling. *J Physiol* **537**, 667–677.

Sridharan M, Adderley SP, Bowles EA, Egan TM, Stephenson AH, Ellsworth ML & Sprague RS (2010). Pannexin 1 is the conduit for low oxygen tension-induced ATP release from human erythrocytes. *Am J Physiol Heart Circ Physiol* **299**, H1146–1152.

Thompson RJ & Macvicar BA (2008). Connexin and pannexin hemichannels of neurons and astrocytes. *Channels (Austin)* **2**, 81–86.

von Kugelgen I (2006). Pharmacological profiles of cloned mammalian P2Y-receptor subtypes. *Pharmacol Ther* **110**, 415–432.

Xu J, Tse FW & Tse A (2003). ATP triggers intracellular $Ca^{2+}$ release in type II cells of the rat carotid body. *J Physiol* **549**, 739–747.

Xu J, Xu F, Tse FW & Tse A (2005). ATP inhibits the hypoxia response in type I cells of rat carotid bodies. *J Neurochem* **92**, 1419–1430.

Yen MR & Saier MH Jr (2007). Gap junctional proteins of animals: the innexin/pannexin superfamily. *Prog Biophys Mol Biol* **94**, 5–14.

Zapata P (2007). Is ATP a suitable co-transmitter in carotid body arterial chemoreceptors? *Respir Physiol Neurobiol* **157**, 106–115.

Zhang M & Nurse CA (2004). $CO_2$/pH chemosensory signaling in co-cultures of rat carotid body receptors and petrosal neurons: role of ATP and ACh. *J Neurophysiol* **92**, 3433–3445.

Zhang M, Zhong H, Vollmer C & Nurse CA (2000). Co-release of ATP and ACh mediates hypoxic signalling at rat carotid body chemoreceptors. *J Physiol* **525**, 143–158.

Zhong H, Zhang M & Nurse CA (1997). Synapse formation and hypoxic signalling in co-cultures of rat petrosal neurones and carotid body type 1 cells. *J Physiol* **503**, 599–612.

## Author contributions

M.Z. performed all the electrophysiological experiments and analysed the data. N.A.P. performed the $Ca^{2+}$ imaging experiments, assisted with the confocal microscopy, and contributed to the figure preparation and editing the manuscript. C.V. performed the RT-PCR and immunofluorescence experiments and assisted with the confocal microscopy. C.A.N. initiated the study, planned and designed all the experiments, and wrote the manuscript. All authors approved the final version of this manuscript.

## Acknowledgements

This work was supported by an operating grant from the Canadian Institutes of Health Research (MOP 12037) to C.A.N. N.A.P. was supported by a Vanier Canada Graduate Scholarship from the Natural Sciences and Engineering Research Council of Canada (NSERC). The Leica TCS SP5 II confocal system and $Ca^{2+}$-imaging rig were purchased with grants from the Canadian Foundation for Innovation-Leaders Opportunity Fund.